
Structural Causal Bottleneck Models

Simon Bing^{*1,2} Jonas Wahl^{*3} Jakob Runge²

Abstract

We introduce structural causal bottleneck models (SCBMs), a novel class of structural causal models. At the core of SCBMs lies the assumption that causal effects between high-dimensional variables only depend on low-dimensional summary statistics, or *bottlenecks*, of the causes. SCBMs provide a flexible framework for task-specific dimension reduction while being estimable via standard, simple learning algorithms in practice. We analyse identifiability in SCBMs, connect them to information bottlenecks in the sense of Tishby & Zaslavsky (2015), and illustrate how to estimate them experimentally. We also demonstrate the benefit of bottlenecks for effect estimation in low-sample transfer learning settings. We argue that SCBMs provide an alternative to existing causal dimension reduction frameworks like causal representation learning or causal abstraction learning.

1. Introduction

A fundamental aim of scientific inquiry is to uncover and quantify causal relationships among complex phenomena, which often span large spaces, long times, or many individuals. For example, neuroscientists study how neuron clusters respond to tasks (Aoi & Pillow, 2018), while climate scientists examine interactions like the El Niño Southern Oscillation, affecting global weather patterns (Timmermann et al., 2018). These phenomena are modeled as high-dimensional random vectors that are consequently simplified, abstracted or transformed.

A popular type of model to formalize causal interactions of random variables is the structural causal model (SCM) (Pearl, 2009). An SCM consists of structural equations $\mathbf{X}_j := m_j(\mathbf{X}_{i_1}, \dots, \mathbf{X}_{i_k}, \boldsymbol{\eta}_j)$, one for each quantity of interest, that describe how each variable is brought about by its *causal parents* $\mathbf{X}_{i_1}, \dots, \mathbf{X}_{i_k}$ and an exogeneous noise term

$\boldsymbol{\eta}_j$ through the mechanism function m_j . Although in most applications of SCMs, the variables \mathbf{X}_j and noise-terms $\boldsymbol{\eta}_j$ are assumed to be one-dimensional, the SCM setup does not necessitate this assumption. However, modeling interactions of high-dimensional vectors \mathbf{X}_j may quickly become infeasible in practice without additional assumptions. Even if the mechanism functions m_j are assumed to be linear and additive, i.e. $\mathbf{X}_j := \sum_{i \in \text{pa}(j)} \mathbf{A}_i^j \mathbf{X}_i + \boldsymbol{\eta}_j$, with matrices \mathbf{A}_i^j , the associated regression tasks require large sample sizes and/or a sufficient degree of regularization to yield reliable outcomes in high dimensions. When estimating causal effects in an SCM, the curse of dimensionality is particularly daunting. The estimation may not only require as input the treatment and outcome variables, but also confounding covariates to remove spurious correlations, increasing the dimension of the input space further.

In this work, we investigate SCMs of high-dimensional random vectors in which the causal variables only depend on their parents through low-dimensional sufficient statistics or *bottlenecks*. That is to say, we assume that for any \mathbf{X}_j and any of its parents \mathbf{X}_i there exists a deterministic bottleneck function b_i^j that maps \mathbf{X}_i to a lower-dimensional variable $\mathbf{Z}_i^j = b_i^j(\mathbf{X}_i)$ such that

$$\mathbf{X}_j := f_j(\mathbf{Z}_{i_1}^j, \dots, \mathbf{Z}_{i_k}^j, \boldsymbol{\eta}_j) \quad (1)$$

depends on its parents only through their bottlenecks. For linear mechanisms, this requirement translates to the assumption that the matrices \mathbf{A}_i^j are of low rank compared to the dimensions of \mathbf{X}_i and \mathbf{X}_j .

The bottleneck assumption is reasonable when modeling causal interactions between high-dimensional phenomena, in which a causal child does not depend on all information encoded in its parents, but on emergent properties—captured for instance by a weighted average or specific system states. To model rainfall patterns over West Africa it may be sufficient to include information on whether El Niño Southern Oscillation (ENSO) is in an El Niño or a La Niña phase rather than modeling the full temperature distribution over the Pacific Ocean. Dimension reduction assumptions have been studied in spatially-aggregated vector autoregressive models of climate teleconnections (Tibau et al., 2022). However, reducing dimensions before estimating causal effects can discard or misidentify important information (Wahl et al., 2024; Ninad et al., 2025). Further, different children

^{*}Equal contribution ¹Technische Universität Berlin
²Department of Computer Science, University of Potsdam
³German Research Center for Artificial Intelligence (DFKI).
Correspondence to: Simon Bing <bing@campus.tu-berlin.de>.

may rely on different aspects of a parent variable. East Asian and South American rainfall patterns may respond to different ENSO region anomalies, calling for *target-dependent* dimension reduction. While *sufficient dimension reduction* has a long history (Izenman, 1975), most approaches focus on linear models with single treatment-outcome pairs (Globerson & Tishby, 2003; Li, 2007; 2018). In addition, with the notable exception of (Aoi & Pillow, 2018), the outcome vector is typically one-dimensional and only the input may be of high-dimensionality.

We formally introduce structural causal bottleneck models (SCBMs), a class of graphical causal models that address the aforementioned shortcomings and provide a flexible framework for targeted dimension reduction for causal effects. We discuss special cases of SCBMs that are not covered in the standard causal inference literature, provide an identifiability result showing the degree to which we can learn the bottleneck variables from data, and establish a connection between SCBMs and the Information Bottleneck method of (Tishby et al., 2000). Finally, we provide experimental evidence to support our theoretical identifiability results, and highlight the benefits of SCBMs in a transfer learning setting where joint observations of all variables are rare.

2. Preliminaries and Definitions

Throughout this work, we fix the following notation. $\mathcal{G} = (\mathcal{V}, \mathcal{E})$ will refer to a directed acyclic graph (DAG) with node set \mathcal{V} and edge set \mathcal{E} . The set of parents of a node $i \in \mathcal{V}$ will be denoted by $\text{pa}(i)$, the set of its children by $\text{ch}(i)$. The set \mathcal{V}_{ex} is the set of exogeneous (i.e. parentless) nodes, while $\mathcal{V}_{end} = \mathcal{V} \setminus \mathcal{V}_{ex}$ is the set of endogeneous nodes. We reserve the letter d to refer to dimensions of vector spaces, e.g. \mathbb{R}^d . We will use the convention that $d = 0$ refers to discrete spaces. Unless specified otherwise, we use the word space in the sense of measurable space, i.e. a set endowed with a σ -algebra. All maps between such spaces are assumed to be measurable.

We recall that a *structural causal model* (SCM) is a tuple $\mathfrak{A} = \langle \mathcal{G}, \mathcal{X}, \mathcal{H}, \boldsymbol{\eta}, \mathcal{M}, \mathbf{X} \rangle$ consisting of

- a DAG $\mathcal{G} = (\mathcal{V}, \mathcal{E})$, a family of *node spaces* $\mathcal{X} = (\mathcal{X}_i)_{i \in \mathcal{V}}$, and a family of *noise spaces* $\mathcal{H} = (\mathcal{H}_i)_{i \in \mathcal{V}}$.
- a family of mutually independent noise terms $\boldsymbol{\eta} = (\boldsymbol{\eta}_i)_{i \in \mathcal{V}}$, where $\boldsymbol{\eta}_i$ takes values in \mathcal{H}_i .
- a family $\mathcal{M} = (m_j)_{j \in \mathcal{V}_{end}}$ of mechanism functions $m_j : \left(\prod_{i \in \text{pa}(j)} \mathcal{X}_i \right) \times \mathcal{H}_j \rightarrow \mathcal{X}_j$;
- a family of random vectors $\mathbf{X} = (\mathbf{X}_i)_{i \in \mathcal{V}}$ that solves

the structural assignments

$$\begin{aligned} \mathbf{X}_j &:= \boldsymbol{\eta}_j, & j \in \mathcal{V}_{ex}, \\ \mathbf{X}_j &:= m_j \left((\mathbf{X}_i)_{i \in \text{pa}(j)}, \boldsymbol{\eta}_j \right), & j \in \mathcal{V}_{end}. \end{aligned}$$

We first define structural causal bottleneck models in full generality. Afterwards, we will add additional assumptions that narrow down the model class

Definition 2.1. A *structural causal bottleneck model* (SCBM) is a tuple $\mathfrak{C} = \langle \mathcal{G}, \mathcal{X}, \mathcal{Z}, \mathcal{H}, \boldsymbol{\eta}, \mathcal{B}, \mathcal{F}, \mathbf{X} \rangle$ consisting of

- a DAG $\mathcal{G} = (\mathcal{V}, \mathcal{E})$, a family of *node spaces* $\mathcal{X} = (\mathcal{X}_i)_{i \in \mathcal{V}}$, and a family of *noise spaces* $\mathcal{H} = (\mathcal{H}_i)_{i \in \mathcal{V}}$.
- a family of mutually independent noise vectors $\boldsymbol{\eta} = (\boldsymbol{\eta}_i)_{i \in \mathcal{V}}$. We assume that each $\boldsymbol{\eta}_i$ takes values in \mathcal{H}_i .
- a family of *bottleneck spaces* $\mathcal{Z} = (\mathcal{Z}_j)_{j \in \mathcal{V}_{end}}$.
- a family $\mathcal{B} = (b_j)_{j \in \mathcal{V}_{end}}$ of surjective *bottleneck functions* $b_j : \prod_{i \in \text{pa}(j)} \mathcal{X}_i \rightarrow \mathcal{Z}_j$.
- a family $\mathcal{F} = (f_j)_{j \in \mathcal{V}_{end}}$ of *effect functions* $f_j : \mathcal{Z}_j \times \mathcal{H}_j \rightarrow \mathcal{X}_j$.
- a family of random vectors $\mathbf{X} = (\mathbf{X}_i)_{i \in \mathcal{V}}$ with joint distribution $P_{\mathbf{X}}$ that solves the structural assignments

$$\begin{aligned} \mathbf{X}_j &:= \boldsymbol{\eta}_j, & j \in \mathcal{V}_{ex}, \\ \mathbf{X}_j &:= f_j \left(b_j \left((\mathbf{X}_i)_{i \in \text{pa}(j)} \right), \boldsymbol{\eta}_j \right), & j \in \mathcal{V}_{end}. \end{aligned}$$

Any SCBM $\mathfrak{C} = \langle \mathcal{G}, \mathcal{X}, \mathcal{Z}, \mathcal{H}, \boldsymbol{\eta}, \mathcal{B}, \mathcal{F}, \mathbf{X} \rangle$ straightforwardly induces an SCM $\mathfrak{A}(\mathfrak{C}) = \langle \mathcal{G}, \mathcal{X}, \boldsymbol{\eta}, \mathcal{M}, \mathbf{X} \rangle$ in the classical sense by defining the mechanism functions as $m_j \left((\mathbf{X}_i)_{i \in \text{pa}(j)}, \boldsymbol{\eta}_j \right) := f_j \left(b_j \left((\mathbf{X}_i)_{i \in \text{pa}(j)} \right), \boldsymbol{\eta}_j \right)$. We call this SCM the *induced SCM*.

Definition 2.2. We call two SCBMs *structurally equivalent* if their induced SCMs coincide.

Since all interventional distributions and the observational distribution of \mathbf{X} are fully determined by the induced SCM, structural equivalent SCBMs share the same interventional distributions (interventional equivalence) and observational distribution (observational equivalence).

To render SCBMs more practical, we need additional assumptions that reduce their degrees of freedom.

In Definition 2.1, the parents of any endogeneous node j are allowed to mix arbitrarily in the bottleneck space \mathcal{Z}_j . A reasonable assumption to impose on such models is that the bottleneck can be subdivided into separate bottlenecks for each parent.

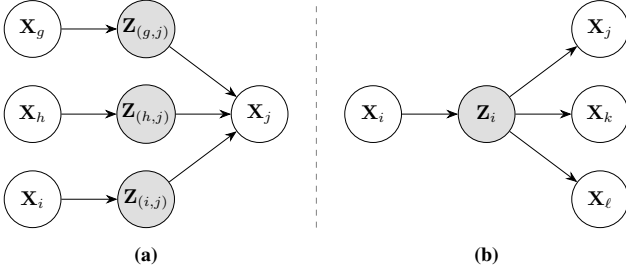


Figure 1. Examples of (a) factored bottleneck and effect functions and (b) intrinsic bottlenecks.

Assumption 2.3. (a) Each bottleneck is *factored* in the sense that \mathcal{Z}_j and b_j can be decomposed as $\mathcal{Z}_j = \prod_{i \in \text{pa}(j)} \mathcal{Z}_{(i,j)}$ and

$$b_j : \prod_{i \in \text{pa}(j)} \mathcal{X}_i \rightarrow \prod_{i \in \text{pa}(j)} \mathcal{Z}_{(i,j)}$$

$$b_j(\mathbf{x}_i)_{i \in \text{pa}(j)} = (b_{(i,j)}(\mathbf{x}_i))_{i \in \text{pa}(j)}$$

with $\dim \mathcal{Z}_{(i,j)} \leq d_i$. In other words, we assume that there is a separate bottleneck space for every parent of the endogenous node j .

(b) Each \mathcal{X}_j is a vector space, and coincides with the noise space $\mathcal{H}_j = \mathcal{X}_j$. Each effect function f_j is factored in the sense that there is a family of maps $f_{(i,j)} : \mathcal{Z}_{(i,j)} \rightarrow \mathcal{X}_j$ such that

$$\mathbf{X}_j := \sum_{i \in \text{pa}(j)} f_{(i,j)}(b_{(i,j)}(\mathbf{X}_i)) + \boldsymbol{\eta}_j.$$

We will call SCBMs for which both (a) and (b) hold *factored SCBMs*. We illustrate Assumption 2.3 (a) and (b) in Figure 1(a).

Intrinsic Structural Bottleneck Models. Factored bottleneck models are still very flexible and allow any variable \mathbf{X}_i to affect its children \mathbf{X}_k , $k \in \text{ch}(i)$, through different bottleneck spaces and functions. The bottleneck variables $\mathbf{Z}_{(i,k)} = b_{(i,k)}(\mathbf{X}_i)$ and $\mathbf{Z}_{(i,k')} = b_{(i,k')}(\mathbf{X}_i)$ do not need to be related and can be of different dimensions for different children $k \neq k'$. On the other hand, we might often believe that there exists an underlying low-dimensional *emergent quantity* that describes the high-dimensional \mathbf{X}_i and its effect on *all* of its targets.

Definition 2.4 (Intrinsic bottlenecks). A node $i \in \mathcal{V}$ in a factored SCBM that has children admits an intrinsic bottleneck if $\mathbf{Z}_{(i,j)} = \mathbf{Z}_i$ and $b_{(i,j)} = b_i$ do not depend on the child j . The effect function $f_{(i,j)}$ is still allowed to depend on j .

We illustrate intrinsic bottlenecks in Figure 1(b).

Equivalence Relations Induced by Bottlenecks. If (i, j) is an edge in the graph \mathcal{G} underlying a factored SCBM \mathfrak{C} , then the function $b_{(i,j)} : \mathcal{X}_i \rightarrow \mathcal{Z}_{(i,j)}$ can be considered a quotient map that induces an equivalence relation on \mathcal{X}_i by declaring two states $\mathbf{x}, \mathbf{x}' \in \mathcal{X}_i$ *bottleneck-equivalent relative to child j* if $b_{(i,j)}(\mathbf{x}) = b_{(i,j)}(\mathbf{x}')$. Thus, two states of the random vector \mathbf{X}_i are bottleneck-equivalent relative to j if both lead to the same state of the bottleneck for child j . As a consequence, two bottleneck-equivalent states (w.r.t. j) are *causally equivalent* w.r.t. the random vector \mathbf{X}_j in the sense of Chalupka et al. (2017), i.e. they satisfy

$$P(\mathbf{X}_j \mid \text{do}(\mathbf{X}_i = \mathbf{x})) = P(\mathbf{X}_j \mid \text{do}(\mathbf{X}_i = \mathbf{x}')).$$

If bottlenecks are assumed intrinsic, then bottleneck-equivalence is no longer relative to a specific child, and bottleneck-equivalent states $\mathbf{x}, \mathbf{x}' \in \mathcal{X}_i$ are causally equivalent for any descendant of i , i.e.

$$P(\mathbf{X}_k \mid \text{do}(\mathbf{X}_i = \mathbf{x})) = P(\mathbf{X}_k \mid \text{do}(\mathbf{X}_i = \mathbf{x}')).$$

for every descendant k of i .

Factorization of the Observational Distribution. In any SCM, the distribution over the observed node vectors $P = P_{\mathbf{X}}$ factorizes according to the graph \mathcal{G} as

$$P(\mathbf{x}) = \prod_{i \in \mathcal{V}} P(\mathbf{x}_i \mid \mathbf{x}_{\text{pa}(i)}).$$

In SCBMs, since \mathbf{X}_i only depends on its parents through the bottleneck variable $\mathbf{Z}_{\text{pa}(i)}$, this can be rewritten as

$$P(\mathbf{x}) = \prod_{i \in \mathcal{V}} P(\mathbf{x}_i \mid \mathbf{z}_{\text{pa}(i)}).$$

In addition, if the SCBM is factored, this expression becomes

$$P(\mathbf{x}) = \prod_{i \in \mathcal{V}} P(\mathbf{x}_i \mid (\mathbf{z}_{(k,i)})_{k \in \text{pa}(i)}).$$

The SCM over the Bottleneck Variables. In a factored SCBM, the bottleneck variables $\mathbf{Z}_{(i,j)}$ can be expressed as

$$\mathbf{Z}_{(i,j)} = b_{(i,j)} \left(\sum_{k \in \text{pa}(i)} f_{(i,k)}(\mathbf{Z}_{(k,i)}) + \boldsymbol{\eta}_i \right).$$

This expression no longer contains any \mathbf{X} -vectors but describes $\mathbf{Z}_{(i,j)}$ fully in terms of other bottleneck nodes and noise terms. In contrast to the model over the \mathbf{X} -vectors, the noise terms in the equations for the $\mathbf{Z}_{(i,j)}$ are no longer guaranteed to be independent. In fact $\mathbf{Z}_{(i,j)}$ and $\mathbf{Z}_{(i,k)}$, $k \neq j$ share the same noise term $\boldsymbol{\eta}_i$, see Appendix B for more.

3. Special Cases and Interpretations

The class of SCBMs is large and allows to model interactions among spatial as well as temporal phenomena as we illustrate below. We also show that SCBMs can be interpreted through the lens of Tishby’s information bottlenecks (Tishby et al., 2000).

Modeling Interactions Between Random Fields. The quantity of interest in geo-spatial modelling are often represented by random fields over some spatial area \mathcal{D} . This spatial area can be a discrete grid or a continuous domain. The random field is a random function over \mathcal{D} , which in the discrete case can be identified with a vector of dimension N , where N is the number of grid points. The spatial structure in such a model is reflected in the correlation structure of the field. For instance, if \mathcal{D} is a discrete grid, a typical assumption is the spatial Markov property, which states that every node X_i , $i \in \mathcal{D}$, is independent of non-adjacent nodes given its neighbors. In continuous random fields, a standard assumption would be that the correlation between two nodes $X(y), X(z)$, $y, z \in \mathcal{D}$, decreases when the spatial distance of y and z increases. An SCBM could for example consist of three random fields of noises η_1, η_2, η_3 over bounded spatial domains $\mathcal{D}_1, \mathcal{D}_2, \mathcal{D}_3$ where fields affect each other only through weighted spatial means, e.g.

$$\begin{aligned} \mathbf{X}_1 &:= \eta_1 \\ \mathbf{X}_2 &:= A \cdot \int_{\mathcal{D}_1} \alpha(y) \mathbf{X}_1(y) dy + \eta_2 \\ \mathbf{X}_3 &:= B \cdot \int_{\mathcal{D}_1} \beta(y) \mathbf{X}_1(y) dy + C \cdot \int_{\mathcal{D}_2} \gamma(z) \mathbf{X}_2(z) dz + \eta_2, \end{aligned}$$

where α, β, γ are normalized to one, e.g. $\int_{\mathcal{D}_1} \alpha(y) dy = 1$. In this case, the spaces are \mathcal{X}_i are function spaces over the respective domains, e.g. $\mathcal{X}_i = L^2(\mathcal{D}_i)$, the bottleneck spaces are one dimensional $\mathcal{Z}_i \cong \mathbb{R}$ and the bottleneck functions are given by the weighted integrals. The effect functions are simple embeddings by multiplication with a constant, e.g. $F_{(1,2)} : \mathcal{Z}_{(1,2)} \rightarrow L^2(\mathcal{D}_2) : z \mapsto Az \cdot \mathbb{1}_{\mathcal{D}_2}$, where $\mathbb{1}_{\mathcal{D}_2}$ denotes the constant function on \mathcal{D}_2 .

Temporal Processes in the Frequency Domain. SCBMs can also model interactions of temporal processes in the frequency domain. For instance, \mathbf{X}_1 and $\mathbf{X}_2 \in L$ may be continuous stochastic processes viewed as random variables with values in $L^2(\mathbb{R}_{\geq 0})$. Their child process \mathbf{Y} may be affected by $\mathbf{X}_1, \mathbf{X}_2$ within at most K frequency components with frequencies $\omega_1, \dots, \omega_K$, see (Schur & Peters, 2024) for an example of this. Thus, the bottleneck maps $b_i : L^2(\mathbb{R}_{\geq 0}) \rightarrow \mathbb{R}^K$ map the processes to the K Fourier coefficients at $\omega_1, \dots, \omega_K$, and the effect function expresses \mathbf{Y} as $\mathbf{Y}_t = \sum_{k=1, \dots, K} (\lambda_1 b_1(\mathbf{x}_1) + \lambda_2 b_2(\mathbf{x}_2)) e^{-it\omega_k} + \eta$ where η is a noise process, for instance a Brownian motion.

SCBMs as Information Bottlenecks Consider two high-dimensional multivariate random variables \mathbf{X}, \mathbf{Y} . The idea of the information bottleneck framework of Tishby et al. (2000) is to find a minimal sufficient statistic for $\mathbf{T} = g(\mathbf{X})$ that captures as much information about the target variable \mathbf{Y} as possible. This goal is captured by the *minimal compression* optimization objective

$$\min_{\mathbf{T} : I(\mathbf{X}, \mathbf{Y}|\mathbf{T})=0} I(\mathbf{X}, \mathbf{T}).$$

The *independence constraint* $I(\mathbf{X}, \mathbf{Y}|\mathbf{T}) = 0$ is equivalent to $I(\mathbf{X}, \mathbf{Y}) = I(\mathbf{T}, \mathbf{Y})$. Note also that the data processing inequality enforces

$$I(g(\mathbf{X}), \mathbf{Y}) \leq I(\mathbf{X}, \mathbf{Y})$$

for any abstraction function g , an information bottleneck is thus nothing but an abstraction of \mathbf{X} that maximizes $I(g(\mathbf{X}), \mathbf{Y})$. This property is used to incorporate the independence constraint as a soft constraint in the joint objective

$$\min_{\mathbf{T}} (I(\mathbf{X}, \mathbf{T}) - \beta I(\mathbf{Y}, \mathbf{T}))$$

with regularization parameter $\beta > 0$. Consider now an intrinsic SCBM over variables \mathbf{X}_i with bottleneck variables $\mathbf{Z}_i = b_i(\mathbf{X}_i)$ for every non-sink node i . i.e.

$$\mathbf{X}_j = f_j(\mathbf{Z}_{i_1}, \dots, \mathbf{Z}_{i_m}) + \eta_j \quad \text{pa}(j) = \{i_1, \dots, i_m\}.$$

Our goal is to produce an optimization objective and constraints to learn the bottleneck variables \mathbf{Z}_i . The minimal compression requirement now means that \mathbf{Z}_i contains the minimal necessary information about \mathbf{X} once \mathbf{X} ’s parents are known, i.e. $\mathbf{Z}_i \in \text{argmin} I(\mathbf{X}_i, \mathbf{Z}_i | \mathbf{Z}_{\text{pa}(i)})$ for all i .

The bottleneck \mathbf{Z}_i is intended to be maximally informative about the children of \mathbf{X}_i provided that all backdoor paths to these children are closed which can be achieved by conditioning on the parental bottlenecks $\mathbf{Z}_{\text{pa}(i)} = \{\mathbf{Z}_k, k \in \text{pa}(i)\}$. Thus, the conditional independence constraint is

$$I(\mathbf{X}_{\text{ch}(i)}, \mathbf{X}_i | \mathbf{Z}_i, \mathbf{Z}_{\text{pa}(i)}) = 0.$$

for non-sink nodes i . By the chain rule for conditional mutual information, this is equivalent to

$$I(\mathbf{X}_{\text{ch}(i)}, \mathbf{Z}_i | \mathbf{Z}_{\text{pa}(i)}) = I(\mathbf{X}_{\text{ch}(i)}, \mathbf{X}_i | \mathbf{Z}_{\text{pa}(i)}).$$

Thus, writing $\mathbf{Z} = (\mathbf{Z}_i)_{i \in \mathcal{V}_{ns}}$, we want to solve the family of optimization objectives

$$\min_{\mathbf{Z} : I(\mathbf{X}_{\text{ch}(i)}, \mathbf{X}_i | \mathbf{Z}_i, \mathbf{Z}_{\text{pa}(i)})=0} I(\mathbf{X}_i, \mathbf{Z}_i | \mathbf{Z}_{\text{pa}(i)}), \quad i \in \mathcal{V}_{ns}.$$

These objectives are linked by the fact that the i -th objective involves not only the bottleneck \mathbf{Z}_i but also the bottlenecks of the parent variables which may be part of other objectives

as well. Instead of solving for \mathbf{Z} globally, it is possible to consider these objectives sequentially along a causal order. To formalize this, define the *causal grading* $\mathcal{V} = \bigsqcup_s \mathcal{V}_s$ where $\mathcal{V}_0 = \mathcal{V}_{ex}$ and $i \in \mathcal{V}_s$ for $s > 0$ if and only if $i \notin \mathcal{V}_q, q < s$ and $\text{pa}(i) \subset \bigsqcup_{q < s} \mathcal{V}_q$. Fixing a causal order (i_1, \dots, i_n) that respects the causal grading allows us to solve the objectives

$$\min_{\mathbf{Z}_i} (I(\mathbf{X}_i, \mathbf{Z}_i | \mathbf{Z}_{\text{pa}(i)}) - \beta_i I(\mathbf{X}_{\text{ch}(i)}, \mathbf{Z}_i | \mathbf{Z}_{\text{pa}(i)}))$$

sequentially along this order since all parental bottlenecks appearing in the i -th equation have been computed as solutions of earlier objectives, see also Appendix D.2.

4. Identifiability

To investigate identifiability of SCBMs, we observe first that it is always possible to create a new, structurally equivalent SCBM from an existing one by inserting invertible mappings on the bottleneck spaces. Lemma 4.2 then shows that for SCMs with additive noise, the converse holds as well. Proofs of the lemmas are provided in Appendix A

Lemma 4.1. *Let $\mathcal{C} = \langle \mathcal{G}, \mathcal{X}, \mathcal{Z}, \boldsymbol{\eta}, \mathcal{B}, \mathcal{F}, \mathbf{X} \rangle$ be an SCBM. Assume that there are invertible maps $\psi_j : \mathcal{Z}_j \rightarrow \mathcal{Z}'_j$ for every endogenous node $j \in \mathcal{V}_{end}$ to some other spaces $\mathcal{Z}' = (\mathcal{Z}'_j)_{j \in \mathcal{V}_{end}}$, and consider the functions $b'_j = \psi_j \circ b_j$ and $f'_j(\cdot, \cdot) = f_j(\psi_j^{-1}(\cdot), \cdot)$. Then $\mathcal{C}' = \langle \mathcal{G}, \mathcal{X}, \mathcal{Z}', \boldsymbol{\eta}, \mathcal{B}', \mathcal{F}', \mathbf{X} \rangle$ with $\mathcal{F}' = (f'_j)_j$ and $\mathcal{B}' = (b'_j)_j$ is structurally equivalent to \mathcal{C} .*

Lemma 4.2. *Let $\mathcal{C} = \langle \mathcal{G}, \mathcal{X}, \mathcal{Z}, \boldsymbol{\eta}, \mathcal{B}, \mathcal{F}, \mathbf{X} \rangle$ and $\mathcal{C}' = \langle \mathcal{G}, \mathcal{X}, \mathcal{Z}', \boldsymbol{\eta}, \mathcal{B}', \mathcal{F}', \mathbf{X} \rangle$ be two SCBMs with additive noises, i.e. $f_j(\mathbf{z}_{\text{pa}(j)}, \eta_j) = f_j(\mathbf{z}_{\text{pa}(j)}) + \eta_j$, and similarly for f'_j . Assume that the functions $\tilde{f}_j : \mathcal{Z}_j \rightarrow \mathcal{X}_j$, $\tilde{f}'_j : \mathcal{Z}'_j \rightarrow \mathcal{X}_j$ are almost surely injective. If \mathcal{C} and \mathcal{C}' are structurally equivalent, there is an invertible function $\psi_j : \mathcal{Z}_j \rightarrow \mathcal{Z}'_j$ such that $b' = \psi \circ b$ and $f'_j = f_j \circ \psi^{-1}$.*

Injectivity of the effect functions is a natural minimality assumption that, together with surjectivity, forces the bottlenecks to be as small as possible without information loss. In the linear case, this guarantees that the rank of the linear map $f_j \circ b_j$ is $\text{rank}(f_j \circ b_j) = \dim \mathcal{Z}_j$ and not lower. In other words, we can always reparametrize the bottleneck space in a different basis if we adapt the bottleneck and effect functions accordingly.

5. Experiments

Estimating SCBMs in Practice The procedure for estimating bottleneck variables from data, given a graph, essentially amounts to fitting a regressor with constraints on the bottleneck dimension. As such, practical estimation of bottleneck variables is flexible enough to accommodate any data modality for which an estimator is available. We do not

require customized loss functions with causal regularizers, as estimation only requires observational data.

Following Assumption 2.3, we consider settings where each parent of an endogenous node has a separate bottleneck. This translates to each edge in \mathcal{G} corresponding to a unique bottleneck space. Recalling that an edge between variables \mathbf{X}_i and \mathbf{X}_j decomposes into a bottleneck function $b_{(i,j)}$, mapping to the bottleneck $\mathbf{Z}_{(i,j)}$, and an effect function $f_{(i,j)}$ that maps back to \mathbf{X}_j , our goal is to recover $b_{(i,j)}$ and $f_{(i,j)}$. We fit an estimator from \mathbf{X}_i to \mathbf{X}_j which recovers an estimate of the joint map $m_{(i,j)} := f_{(i,j)} \circ b_{(i,j)} : \mathcal{X}_i \times \mathcal{H}_j \rightarrow \mathcal{X}_j$. Any valid conditioning set for estimating the causal effect $\mathbf{X}_i \rightarrow \mathbf{X}_j$ is also valid for estimating this joint map. As per Lemma 4.2, from the estimated joint map $\hat{m}_{(i,j)}$ we recover $b_{(i,j)}$ and $f_{(i,j)}$ up to an invertible map $\psi_{(i,j)}$, i.e., $\hat{b}_{(i,j)} := \psi_{(i,j)} \circ b_{(i,j)}$ and $\hat{f}_{(i,j)} := f_{(i,j)} \circ \psi_{(i,j)}^{-1}$. In the linear case, recovering $\hat{f}_{(i,j)}$ and $\hat{b}_{(i,j)}$ from $\hat{m}_{(i,j)}$ amounts to finding a matrix factorization in terms of factors with specified ranks, in the nonlinear case we recover the factorization by means of an encoder-decoder architecture. See Appendix D.2 for a detailed account of the estimation procedure. Code to reproduce our experiments is available <https://github.com/simonbing/StructuralCausalBottleneckModels>.

5.1. Identifiability

Setup. Our first set of experiments aims to validate our identifiability theory presented in Section 4. To do so, we sample data from a joint distribution induced by an SCBM \mathcal{C} , estimating all bottleneck variables and measuring how well these estimated variables $\hat{\mathbf{Z}}$ recover the ground-truth bottlenecks \mathbf{Z} . We randomly sample SCBMs with number of vertices $|\mathcal{V}|$, internal node dimension $d_{\mathbf{X}}$, bottleneck dimension $d_{\mathbf{Z}}$ and linear or nonlinear mechanisms. See Appendix D.1 for all details on the data generating process. We vary these parameters to study how well bottlenecks can be recovered across a diverse range of settings. Default settings are $|\mathcal{V}| = 10$, $d_{\mathbf{X}} = 5$, $d_{\mathbf{Z}} = 2$ and $n = 30000$ for linear and $n = 50000$ for nonlinear mechanisms, respectively.

Since our notion of identifiability amounts to estimating the ground-truth bottlenecks up to a bijection (cf. Lemma 4.2), we fit an estimator between each ground-truth $\mathbf{Z}_{(i,j)}$ and its estimate $\hat{\mathbf{Z}}_{(i,j)}$ in *both* directions and use the average of the R^2 of both fits as our metric. Considering both directions is required as we wish to test equivalence up to a bijection; a surjective map between $\mathbf{Z}_{(i,j)}$ and $\hat{\mathbf{Z}}_{(i,j)}$ would achieve a perfect score in one direction, but not in the other. The final score we report is the mean of this metric across all nodes.

Results. In linear SCBMs, we successfully recover bottleneck variables across all settings. Performance improves

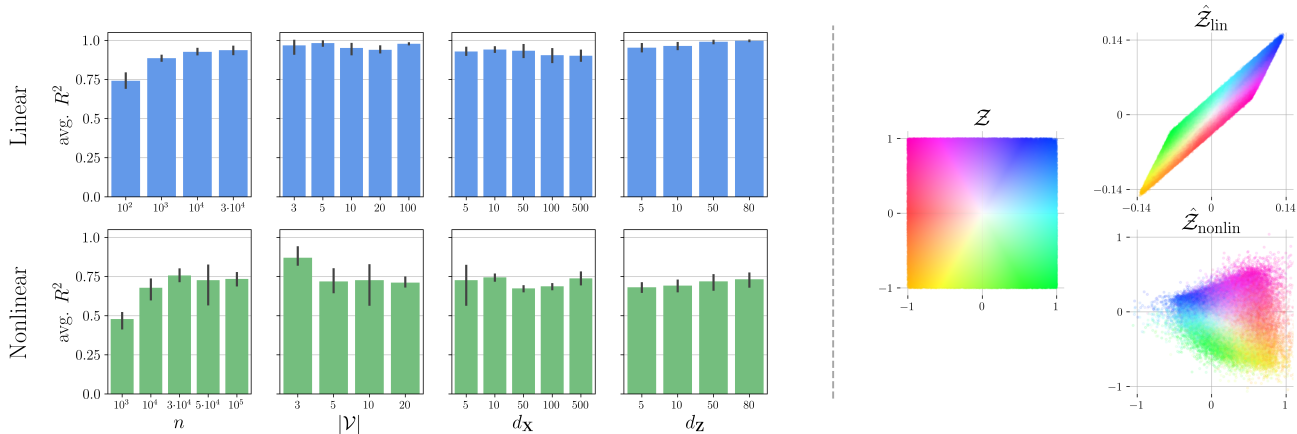


Figure 2. Left: Results of the identifiability experiments across various settings. We report the mean average R^2 along with its standard deviation. The top row shows results for linear SCBMs and the bottom row for nonlinear SCBMs. High average R^2 scores across models and settings indicate that we successfully learn the bottleneck variables up to a bijection. **Right:** Visualization of learned bottleneck spaces $\hat{\mathcal{Z}}$ w.r.t. to the ground-truth space \mathcal{Z} . For both linear and nonlinear cases, $\hat{\mathcal{Z}}$ corresponds to \mathcal{Z} up to a (linear or nonlinear) bijection.

quickly with sample size, saturating around $n = 10000$, and remains strong as the number of nodes increases, suggesting minimal error propagation. As $d_{\mathbf{X}}$ increases, R^2 scores slightly drop due to greater compression demands. When varying $d_{\mathbf{Z}}$ (with $d_{\mathbf{X}} = 100$), performance stays high and converges to perfect as $d_{\mathbf{Z}}$ approaches $d_{\mathbf{X}}$, as expected.

For nonlinear SCBMs, scores are lower, though not beyond what is expected from a harder estimation problem. Nonlinear mechanisms require more samples, with performance saturating around $n = 30000$. Increasing $|\mathcal{V}|$ leads to decreased performance, indicating larger error propagation than in the linear case, though this does not cause catastrophic failure.¹ Larger $d_{\mathbf{X}}$ does not affect performance. When varying $d_{\mathbf{Z}}$ (again with $d_{\mathbf{X}} = 100$), performance slowly increases as $d_{\mathbf{Z}}$ approaches $d_{\mathbf{X}}$.

We also plot exemplary learned bottleneck spaces in Figure 2, illustrating the invertible transformation ψ up to which we recover bottleneck variables (cf. Lemma 4.2). In the linear case, we see the learned space transformed by rotation, scaling, and shearing, i.e., an affine transformation. For nonlinear mechanisms, the map from ground-truth to learned space is a smooth bijection preserving local structure. Additional visualizations are provided in Appendix C.

5.2. Misspecification

Setup In the previous experiment, we assumed knowledge of the ground-truth bottleneck dimension $d_{\mathbf{Z}}$, an assumption that we will now drop. To study the effect of varying the

¹Experiments for $|\mathcal{V}| = 100$ exceeded our compute budget, as such graphs have ~ 3500 edges, each requiring a neural network for bottleneck estimation. In practice, one would estimate only the bottlenecks needed for a specific query.

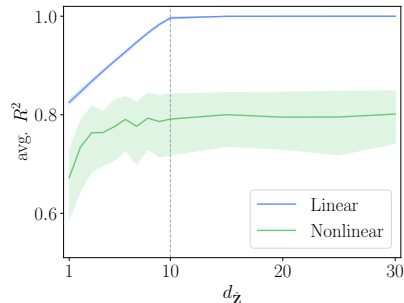


Figure 3. Mean average R^2 and 95% confidence interval of identifying bottlenecks with misspecified assumed bottleneck dimension $d_{\hat{\mathbf{Z}}}$. The dashed vertical line indicates the ground-truth bottleneck dimension. For both linear and nonlinear settings, the metric increase until it saturates at $d_{\hat{\mathbf{Z}}} = d_{\mathbf{Z}}$, indicating that the true bottleneck dimension is a lower bound for identifiability.

assumed bottleneck dimension of our estimator, we consider a cause-effect pair, both with internal dimension $d_{\mathbf{X}}$ and an associated bottleneck variable with dimension $d_{\mathbf{Z}}$. We set $d_{\mathbf{X}} = 50$ for the linear, $d_{\mathbf{X}} = 100$ for the nonlinear case and $d_{\mathbf{Z}} = 10$ for both. Starting from $d_{\hat{\mathbf{Z}}} = 1$, we increase the bottleneck dimension assumed by the estimator.

Results For both linear and nonlinear mechanisms, our identifiability metric increases with bottleneck dimension until saturating at $d_{\hat{\mathbf{Z}}} = d_{\mathbf{Z}}$ (Figure 3). This is expected: the ground-truth $d_{\mathbf{Z}}$ is the minimum capacity needed to recover all bottleneck information. More compression leads to information loss, but less compression does not hurt. This highlights a key practical difference to approaches like CRL, where assuming the correct latent dimension is critical. For bottleneck models, the ground-truth dimension is a lower bound, whereas for CRL, both under- and overestimating

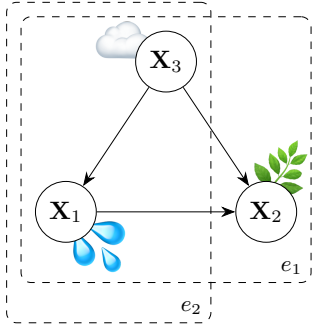


Figure 4. Graph of the SCBM used for the transfer learning experiments. We assume that samples from the environment e_1 , where all variables are jointly observed, are relatively scarce compared to the number of samples of environment e_2 , where we only jointly observe X_1 and X_3 .

the latent dimension compromises identifiability guarantees.

5.3. Transfer Learning

Setup. Consider a three variable SCBM with graph \mathcal{G} depicted in Figure 4. Our query is the effect of X_1 on X_2 , which is confounded by X_3 . We assume access to few samples of the joint distribution X_1, X_2, X_3 , but orders of magnitude more samples of X_1, X_3 . This is related to the causal marginal problem (Gresele et al., 2022), where samples come from different environments with varying variable coverage. As motivation, consider X_1 as rainfall, X_2 as vegetation growth, and X_3 as cloud coverage. Measurements of X_1 and X_3 may come from a local station collecting samples at high frequency, while joint measurements including vegetation are collected from a satellite at much lower frequency. Estimating the effect $X_1 \rightarrow X_2$ requires conditioning on the confounder X_3 , which given high node dimensionality and small joint sample size, is likely ill-conditioned.

We study whether abundant data from X_1, X_3 can improve effect estimation in this low sample regime. Specifically, we use these samples to estimate $\hat{Z}_{(3,1)}$, which can replace X_3 for conditioning since it blocks the confounding path (see Appendix B). Since bottleneck variables have lower dimension than observed variables, using them for conditioning should be beneficial when joint samples of X_1, X_2, X_3 are scarce but observations of X_1, X_3 are abundant—the low-dimensional bottlenecks yield a larger effective sample size. For the linear case we set $d_{\mathbf{X}} = 50$ and $d_{\mathbf{Z}} = 2$; for the nonlinear case $d_{\mathbf{X}} = 500$. We use $n = 20000$ samples to estimate the bottleneck, then study effect estimation performance for varying joint sample sizes.

Results. For linear models—as shown in Figure 5—in the very low sample regime, using the bottleneck as conditioning variables provides a substantial benefit in terms of

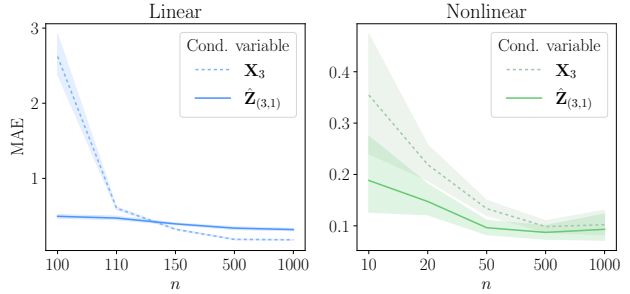


Figure 5. Mean absolute error (MAE) and 95% confidence interval of estimating the effect $X_1 \rightarrow X_2$ using different conditioning variables. For both linear and nonlinear SCBMs, using the estimated bottleneck variable is beneficial for small sample sizes.

incurred error w.r.t. directly conditioning on the observed variable. This benefit subsides as the sample size increases, but nevertheless highlights the settings where bottleneck variables may be useful in practice. For nonlinear models, the same holds, however only becoming pronounced for larger internal node dimension $d_{\mathbf{X}}$. A connection to pursue in future work is how the gains of using bottleneck variables over observed high-dimensional conditioning sets fits in with the literature of optimal adjustment sets (Runge, 2021; Henckel et al., 2022). It would be interesting to study cases where conditioning on an optimal, high-dimensional set is possible, as well as on a lower-dimensional, suboptimal bottleneck set and formalizing their tradeoff.

6. Related Work

Causal Representation Learning. Although we also learn representations of high-dimensional observations, our approach differs from canonical causal representation learning (CRL) approaches (Schölkopf et al., 2021; Brehmer et al., 2022; Ahuja et al., 2023; Lippe et al., 2022; 2023a;b; Squires et al., 2023; Buchholz et al., 2023; Liang et al., 2023; Varıcı et al., 2023; Bing et al., 2024; Lachapelle et al., 2024; von Kügelgen et al., 2024; Yao et al., 2024) in key ways. Instead of mapping observations to SCM nodes, we learn *multiple* maps tied to mechanisms between known (vector-valued) SCM nodes. Unlike most CRL methods that seek latent variables up to permutation and rescaling, we allow a broader class of invertible transformations for identifiability. Additionally, while CRL assumes invertible maps, we focus on surjective maps to enable true dimension reduction by discarding irrelevant observational details.

CRL aims to recover a latent low-dimensional SCM including its constituting variables. In contrast, learning bottlenecks in an SCBM is focused on causal effect estimation. We learn representations assuming a known graph and target a specific downstream causal query. Defining causal representations by their usefulness for downstream tasks,

rather than recovering a single postulated ground-truth latent model, has been proposed as a step forward for CRL (Jørgensen et al., 2025), and our targeted approach aligns with this view.

Causal Abstractions. Our work is related to causal abstraction learning, but *what* we abstract is different from existing approaches. Common approaches abstract causal models as a whole (Zennaro et al., 2023; Felekis et al., 2024; Xia & Bareinboim, 2024; Massidda et al., 2024; D’Acunto et al., 2025), while our notion of abstraction is a within-model operation that reduces a random vector to the essentials needed for downstream effect estimations.

An approach closely related to ours is the causal feature learning method proposed by Chalupka et al. (2017), which learns to partition the spaces of a cause-effect pair to extract high-level features from low-level observations. The SCBM framework extends this idea to settings with more than two variables and allows for continuous high-level variables (bottlenecks), as opposed to only permitting discrete variables as a result of a clustering operation.

The Causal Information Bottleneck (CIB) (Simoes et al., 2024) seeks a representation for a specific causal query, but differs from our approach in its problem setting and method. The CIB framework focuses on a single cause-effect pair which must be identifiable via the backdoor criterion, while we handle arbitrary acyclic graphs. Simoes et al. (2024) extend the Information Bottleneck Lagrangian of Tishby et al. (2000) to trade off compression and what they call “causal control” via a constrained optimization, whereas we assume a data generating process that conceptualizes optimal low-dimensional representations directly and enables bottleneck estimation through regression or likelihood-based losses. The CIB method requires access to all conditional probability distributions, as it must compute $p(\mathbf{Y} \mid \text{do}(\mathbf{X} = \mathbf{x}))$, while we use only observational data and graph structure. Additionally, CIB assumes discrete variables; we allow both discrete and continuous.

Dimension Reduction. Principle component analysis (PCA) (Pearson, 1901) and similar dimension reduction techniques can be understood to represent the opposing side of a trade-off between training effort required before application and guarantees over retained relevant information for a downstream task. PCA does not need to be fit to a specific setting, but may also discard data relevant to a downstream task. In our framework, we do require additional data to fit an estimator of a given bottleneck, but we gain guarantees of the compressed representation being optimal for describing the specific mechanism of interest.

In a setting with only one regressor \mathbf{X} and one regressand \mathbf{Y} , the task of finding an appropriate bottleneck variable

is known as sufficient dimension(ality) reduction (Globerson & Tishby, 2003; Li, 2007; 2018). If in addition the relationship of \mathbf{X} and \mathbf{Y} is assumed linear, *reduced-rank regression* (Izenman, 1975) implicitly assumes the existence of a low-dimensional bottleneck variable by restricting the rank of the effect matrix.

Connections to Matching. Matching is a prominent technique for estimating the effect of an (often binary) treatment variable T on an outcome Y in the presence of confounding covariates X_1, \dots, X_k . Roughly speaking, the idea behind matching is to pair treated and untreated units that are as similar as possible in terms of their covariate values. *Exact matching*, that is, matching directly in the covariate space $\mathcal{X}_1 \times \dots \times \mathcal{X}_k$, for instance by measuring the Euclidean distance of the covariate values of the units, is often unfeasible if the sample size is small compared to the number of covariates. In this case, matching is commonly done by measuring the similarity of units in a bottleneck space. For instance, *propensity score matching* declares units similar that are close in propensity score $e(\mathbf{x}) = P(T = 1 \mid \mathbf{X} = \mathbf{x})$ (Rosenbaum & Rubin, 1983) which in our terminology is a $[0, 1]$ -valued bottleneck between the covariates and the treatment. *Coarsened exact matching* (Blackwell et al., 2009) interpolates between exact matching and the propensity score by operating in a coarser bottleneck space.

7. Outlook

We introduce Structural Causal Bottleneck Models, a novel family of graphical causal models for vector-valued variables. The assumption at the heart of SCBMs is that effects between high-dimensional variables can be equivalently described using low-dimensional bottleneck variables. We formalize this idea and provide an identifiability result that characterizes when these bottlenecks can be learned from data. We provide a proof-of-concept estimation method to validate our theory and underline the benefit of SCBMs for transfer learning. Our estimation method is relatively simple in comparison to most CRL and causal abstraction approaches. Our hope is that this provides some robustness to assumption violations in real data, which seem to negatively affect these methods (Gamella* et al., 2025). How SCBMs map to application problems was beyond the scope of this first, introductory work and remains to be studied.

Future research directions include developing application specific estimators, as our methodology generally permits fitting any model compatible with in- and output data modalities, without requiring a bespoke causal loss. Formally characterizing the optimality gains that bottleneck variables as conditioning sets provide in low-sample settings also presents a promising future direction of study. Finally, understanding if and how methods for causal discovery could

exploit the bottleneck assumption to learn the graph we assume to know is a promising premise for future work.

Acknowledgements

S.B. and J.R. received funding for this project from the European Research Council (ERC) Starting Grant CausalEarth under the European Union’s Horizon 2020 research and innovation program (Grant Agreement No. 948112). S.B. received support from the German Academic Scholarship Foundation. J.W. received support from the German Federal Ministry of Education and Research (BMBF) as part of the project MAC-MERLin (Grant Agreement No. 01IW24007). This work used resources of the Deutsches Klimarechenzentrum (DKRZ) granted by its Scientific Steering Committee (WLA) under project ID 1083.

Impact Statement

This paper presents a novel type of causal graphical model. Such models may play a role in Machine Learning and Artificial Intelligence applications in the future, but as the work presented here amounts to basic research, we feel there are no direct ethical or societal consequences that should be highlighted.

References

- Ahuja, K., Mahajan, D., Wang, Y., and Bengio, Y. Interventional Causal Representation Learning. In *Proceedings of the 40th International Conference on Machine Learning*, pp. 372–407, 2023.
- Aoi, M. and Pillow, J. W. Model-based targeted dimensionality reduction for neuronal population data. In *Advances in Neural Information Processing Systems*, volume 31, 2018.
- Bing, S., Ninad, U., Wahl, J., and Runge, J. Identifying Linearly-Mixed Causal Representations from Multi-Node Interventions. In *Proceedings of the Third Conference on Causal Learning and Reasoning*, pp. 843–867, 2024.
- Bjerhammar, A. Application of calculus of matrices to method of least squares: with special reference to geodesic calculations. *Kungl. Tekniska Högskolans handlingar*, 49, 1951.
- Blackwell, M., Iacus, S., King, G., and Porro, G. cem: Coarsened exact matching in stata. *The stata journal*, 9(4):524–546, 2009.
- Bradbury, J., Frostig, R., Hawkins, P., Johnson, M. J., Leary, C., Maclaurin, D., Necula, G., Paszke, A., VanderPlas, J., Wanderman-Milne, S., and Zhang, Q. JAX: composable transformations of Python+NumPy programs, 2018. URL <http://github.com/jax-ml/jax>.
- Brehmer, J., de Haan, P., Lippe, P., and Cohen, T. S. Weakly supervised causal representation learning. In *Advances in Neural Information Processing Systems*, 35, pp. 38319–38331, 2022.
- Buchholz, S., Rajendran, G., Rosenfeld, E., Aragam, B., Schölkopf, B., and Ravikumar, P. Learning linear causal representations from interventions under general nonlinear mixing. In *Advances in Neural Information Processing Systems*, volume 36, pp. 45419–45462, 2023.
- Chalupka, K., Eberhardt, F., and Perona, P. Causal feature learning: an overview. *Behaviormetrika*, 44:137–164, 2017.
- D’Acunto, G., Zennaro, F. M., Felekis, Y., and Di Lorenzo, P. Causal abstraction learning based on the semantic embedding principle. *arXiv preprint arXiv:2502.00407*, 2025.
- Erdős, P. and Rényi, A. On Random Graphs I. *Publicationes Mathematicae Debrecen*, 6:290–297, 1959.
- Felekis, Y., Zennaro, F. M., Branchini, N., and Damoulas, T. Causal optimal transport of abstractions. In *Proceedings of the Third Conference on Causal Learning and Reasoning*, pp. 462–498, 2024.
- Gamella*, J. L., Bing*, S., and Runge, J. Sanity checking causal representation learning on a simple real-world system. *arXiv preprint arXiv:2502.20099*, 2025. *equal contribution.
- Globerson, A. and Tishby, N. Sufficient dimensionality reduction. *Journal of Machine Learning Research*, 3: 1307–1331, 2003.
- Gresele, L., Von Kügelgen, J., Kübler, J., Kirschbaum, E., Schölkopf, B., and Janzing, D. Causal inference through the structural causal marginal problem. In *Proceedings of the 39th International Conference on Machine Learning*, pp. 7793–7824, 2022.
- Henckel, L., Perković, E., and Maathuis, M. H. Graphical Criteria for Efficient Total Effect Estimation Via Adjustment in Causal Linear Models. *Journal of the Royal Statistical Society Series B: Statistical Methodology*, 84(2):579–599, 2022.
- Izenman, A. J. Reduced-rank regression for the multivariate linear model. *Journal of multivariate analysis*, 5(2):248–264, 1975.
- Jørgensen, F. H., Gresele, L., and Weichwald, S. What is causal about causal models and representations? *arXiv preprint arXiv:2501.19335*, 2025.

- Lachapelle, S., López, P. R., Sharma, Y., Everett, K., Priol, R. L., Lacoste, A., and Lacoste-Julien, S. Nonparametric Partial Disentanglement via Mechanism Sparsity: Sparse Actions, Interventions and Sparse Temporal Dependencies. *arXiv preprint arXiv:2401.04890*, 2024.
- Lauritzen, S. L. and Richardson, T. S. Chain graph models and their causal interpretations. *Journal of the Royal Statistical Society Series B: Statistical Methodology*, 64(3):321–348, 2002.
- Li, B. *Sufficient dimension reduction: Methods and applications with R*. Chapman and Hall/CRC, 2018.
- Li, L. Sparse sufficient dimension reduction. *Biometrika*, 94(3):603–613, 2007.
- Liang, W., Kekić, A., von Kügelgen, J., Buchholz, S., Besserve, M., Gresele, L., and Schölkopf, B. Causal component analysis. In *Advances in Neural Information Processing Systems*, volume 36, 2023.
- Lippe, P., Magliacane, S., Löwe, S., Asano, Y. M., Cohen, T., and Gavves, S. CITRIS: Causal identifiability from temporal intervened sequences. In *Proceedings of the 39th International Conference on Machine Learning*, Proceedings of Machine Learning Research, pp. 13557–13603, 2022.
- Lippe, P., Magliacane, S., Löwe, S., Asano, Y. M., Cohen, T., and Gavves, E. Causal representation learning for instantaneous and temporal effects in interactive systems. In *International Conference on Learning Representations*, 2023a.
- Lippe, P., Magliacane, S., Löwe, S., Asano, Y. M., Cohen, T., and Gavves, E. BISCUIT: Causal Representation Learning from Binary Interactions. In *Proceedings of the 39th Conference on Uncertainty in Artificial Intelligence*, pp. 1263–1273, 2023b.
- Loshchilov, I. and Hutter, F. Decoupled weight decay regularization. In *International Conference on Learning Representations*, 2019.
- Massidda, R., Magliacane, S., and Bacciu, D. Learning causal abstractions of linear structural causal models. In *Proceedings of the 40th Conference on Uncertainty in Artificial Intelligence*, 2024.
- Moore, E. H. On the reciprocal of the general algebraic matrix. *Bulletin of the american mathematical society*, 26:294–295, 1920.
- Ninad, U., Wahl, J., Gerhardus, A., and Runge, J. Causal discovery on vector-valued variables and consistency-guided aggregation. *arXiv preprint arXiv:2505.10476*, 2025.
- Pearl, J. *Causality*. Cambridge University Press, 2009.
- Pearson, K. Liii. on lines and planes of closest fit to systems of points in space. *The London, Edinburgh, and Dublin philosophical magazine and journal of science*, 2(11):559–572, 1901.
- Penrose, R. A generalized inverse for matrices. *Mathematical Proceedings of the Cambridge Philosophical Society*, 51(3):406–413, 1955.
- Rosenbaum, P. R. and Rubin, D. B. The central role of the propensity score in observational studies for causal effects. *Biometrika*, 70(1):41–55, 1983.
- Runge, J. Necessary and sufficient graphical conditions for optimal adjustment sets in causal graphical models with hidden variables. *Advances in Neural Information Processing Systems*, 34:15762–15773, 2021.
- Schölkopf, B., Locatello, F., Bauer, S., Ke, N. R., Kalchbrenner, N., Goyal, A., and Bengio, Y. Toward Causal Representation Learning. *Proceedings of the IEEE*, 109(5):612–634, 2021.
- Schur, F. and Peters, J. Decor: Deconfounding time series with robust regression. *arXiv preprint arXiv:2406.07005*, 2024.
- Simoes, F. N., Dastani, M., and van Ommen, T. Optimal causal representations and the causal information bottleneck. *arXiv preprint arXiv:2410.00535*, 2024.
- Squires, C., Seigal, A., Bhate, S. S., and Uhler, C. Linear Causal Disentanglement via Interventions. In *Proceedings of the 40th International Conference on Machine Learning*, pp. 32540–32560, 2023.
- Tibau, X.-A., Reimers, C., Gerhardus, A., Denzler, J., Eyring, V., and Runge, J. A spatiotemporal stochastic climate model for benchmarking causal discovery methods for teleconnections. *Environmental Data Science*, 1:e12, 2022.
- Timmermann, A., An, S.-I., Kug, J.-S., Jin, F.-F., Cai, W., Capotondi, A., Cobb, K. M., Lengaigne, M., McPhaden, M. J., Stuecker, M. F., et al. El niño–southern oscillation complexity. *Nature*, 559(7715):535–545, 2018.
- Tishby, N. and Zaslavsky, N. Deep learning and the information bottleneck principle. In *2015 IEEE Information Theory Workshop (ITW)*, pp. 1–5. Ieee, 2015.
- Tishby, N., Pereira, F. C., and Bialek, W. The information bottleneck method. *arXiv preprint physics/0004057*, 2000.

- Varıcı, B., Acartürk, E., Shanmugam, K., Kumar, A., and Tajer, A. Score-based Causal Representation Learning with Interventions. *arXiv preprint arXiv:2301.08230*, 2023.
- von Kügelgen, J., Besserve, M., Wendong, L., Gresele, L., Kekić, A., Bareinboim, E., Blei, D., and Schölkopf, B. Nonparametric identifiability of causal representations from unknown interventions. In *Advances in Neural Information Processing Systems*, volume 36, 2024.
- Wahl, J., Ninad, U., and Runge, J. Foundations of causal discovery on groups of variables. *Journal of Causal Inference*, 12(1):20230041, 2024.
- Xia, K. and Bareinboim, E. Neural causal abstractions. In *Proceedings of the AAAI Conference on Artificial Intelligence*, volume 38, pp. 20585–20595, 2024.
- Yao, D., Xu, D., Lachapelle, S., Magliacane, S., Taslakian, P., Martius, G., von Kügelgen, J., and Locatello, F. Multi-view causal representation learning with partial observability. In *International Conference on Learning Representations*, 2024.
- Zennaro, F. M., Drávucz, M., Apachitei, G., Widanage, W. D., and Damoulas, T. Jointly learning consistent causal abstractions over multiple interventional distributions. In *Proceedings of the Second Conference on Causal Learning and Reasoning*, pp. 88–121, 2023.

A. Proofs

Proof of Lemma 4.1. The result follows directly from the fact that the structural equations in both models coincide:

$$\begin{aligned}
 m'_j((\mathbf{X}_i)_{i \in \text{pa}(j)}, \boldsymbol{\eta}_j) &= f'_j(b'_j((\mathbf{X}_i)_{i \in \text{pa}(j)}), \boldsymbol{\eta}_j) \\
 &= f'_j(\psi_j^{-1}(\psi_j(b_j((\mathbf{X}_i)_{i \in \text{pa}(j)}))) \cdot \boldsymbol{\eta}_j) \\
 &= f_j(b_j((\mathbf{X}_i)_{i \in \text{pa}(j)}), \boldsymbol{\eta}_j) \\
 &= m_j((\mathbf{X}_i)_{i \in \text{pa}(j)}, \boldsymbol{\eta}_j)
 \end{aligned}$$

□

Proof of Lemma 4.2. Since the models are structurally equivalent and the noise terms are the same in both models, it follows directly that $f_j \circ b_j = f'_j \circ b'_j$ $P_{\mathbf{X}}$ -almost surely. In particular the maps f_j, f'_j have the same range, so that the map $\psi_j = f'_j \circ b'_j \circ f_j^{-1}$ is well-defined and has the desired properties. □

B. An SCM over the Bottleneck Variables

Consider a factored SCBM in the sense of Assumption 2.3 with node variables \mathbf{X}_i , $i \in \mathcal{V}$, associated exogenous noise terms $\boldsymbol{\eta}_i$, $i \in \mathcal{V}$ and bottleneck variables $\mathbf{Z}_{(i,j)}$, $(i,j) \in \mathcal{E}$. For each $\mathbf{Z}_{(i,j)} = b_{(i,j)}(\mathbf{X}_i)$ we can write a new structural equation

$$\mathbf{Z}_{(i,j)} := h_{(i,j)}((\mathbf{Z}_{(k,i)})_{k \in \text{pa}(i)}, \boldsymbol{\eta}_i)$$

where $h_{(i,j)}((\mathbf{Z}_{(k,i)})_{k \in \text{pa}(i)}, \boldsymbol{\eta}_i) = b_{(i,j)}\left(\sum_{k \in \text{pa}(i)} f_{(k,i)}(\mathbf{Z}_{(k,i)}) + \boldsymbol{\eta}_i\right)$. Note that the noise term in this equation is no longer additive and that bottleneck variables $\mathbf{Z}_{(i,j)}, \mathbf{Z}_{(i,l)}$ with the same parent \mathbf{X}_i share the same exogenous noise term $\boldsymbol{\eta}_i$. This does not imply that the shared noise terms necessarily induce dependence: for instance, the noise term may be two-dimensional and $b_{(i,j)}$ may only depend on the first component while $b_{(i,k)}$ depends on the second. Nevertheless, if we consider the SCM consisting of all structural equations for the bottleneck variables, generically, the underlying causal graph of this SCM can no longer be represented by a DAG, as the exogenous noise terms in this SCM need not be independent. Instead, the observational distribution over the bottlenecks is Markovian with respect to a mixed graph \mathcal{D} containing bidirected edges $\mathbf{Z}_{(i,j)} \leftrightarrow \mathbf{Z}_{(i,l)}$ as well as directed edges $\mathbf{Z}_{(k,i)} \rightarrow \mathbf{Z}_{(i,j)}$. We can assess adjustment claims using these new structural equations. For instance, if we want to estimate the causal effect of a treatment $\mathbf{T} = \mathbf{X}_k$ on an outcome $\mathbf{O} = \mathbf{X}_l$ and \mathbf{X}_i blocks a backdoor path $\mathbf{T} \leftarrow \dots \mathbf{X}_s \leftarrow \mathbf{X}_i \rightarrow \mathbf{X}_{s'} \rightarrow \dots \rightarrow \mathbf{O}$ in the original DAG, then either of the bottleneck variables $\mathbf{Z}_{(i,s)}$ or $\mathbf{Z}_{(i,s')}$ block the induced backdoor path $\mathbf{T} \leftarrow \dots \mathbf{X}_s \leftarrow \mathbf{Z}_{(i,s)} \leftrightarrow \mathbf{Z}_{(i,s')} \rightarrow \mathbf{X}_{s'} \rightarrow \dots \rightarrow \mathbf{O}$ in the mixed graph \mathcal{D} underlying the SCM in which the equation for \mathbf{X}_i was replaced by the equations for its bottlenecks. For frontdoor adjustment, the situation is more complicated. If we would like to estimate a direct effect $\mathbf{T} \rightarrow \mathbf{O}$ and need to close a frontdoor path $\mathbf{T} \rightarrow \mathbf{X}_1 \rightarrow \dots \rightarrow \mathbf{X}_s \rightarrow \mathbf{O}$, we are not allowed to use the bottleneck on the edge $\mathbf{T} \rightarrow \mathbf{X}_1$ for adjustment as it might be correlated (or even equal) to the bottleneck on the edge $\mathbf{T} \rightarrow \mathbf{O}$ which we like to estimate. We describe a procedure to circumvent this issue in the paragraph *Estimating All Bottlenecks* of Appendix D.2.

C. Additional Identifiability Visualizations

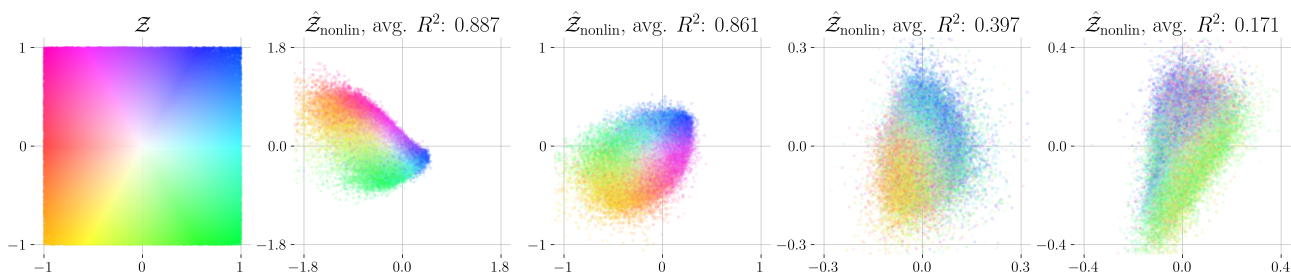


Figure 6. Visualizations of maps from ground truth bottleneck space \mathcal{Z} (first plot) to different learned bottleneck spaces $\hat{\mathcal{Z}}_{\text{nonlin}}$. The second and third plots show examples of successfully identified bottlenecks, as visualized by the smooth, structure preserving bijections from ground-truth to learned bottleneck spaces. We additionally show the identifiability metric, which in both cases is close to one. The third and fourth plots show examples where identifiability is not achieved (by not training to convergence). For such non-identified cases, the learned map is not a bijection and the local structure of the ground-truth bottleneck space is not preserved. The low R^2 metric in these failure cases further reflects non-identification of the ground-truth bottleneck.

D. Additional Experimental Details

D.1. General Data Generation Process

We generate data by first randomly sampling an SCBM \mathcal{C} and then drawing n samples from the joint distribution induced by \mathcal{C} . To sample an SCBM, we set the number of vertices \mathcal{V} , the internal dimension of the nodes $d_{\mathbf{X}}$ and the dimension of the bottleneck spaces $d_{\mathbf{Z}}$. With these fixed parameters, first the graph \mathcal{G} is sampled from an Erdős–Rényi model (Erdős & Rényi, 1959) with edge probability $p = 0.7$. Then, for each node \mathbf{X}_j we sample the distribution of its respective noise term from a Markov Random Field whose joint distribution is a Gaussian and internal dynamics are described by the Langevin diffusion (Lauritzen & Richardson, 2002) with dimension $d_{\mathbf{X}}$. For each edge in \mathcal{G} , we randomly sample both a bottleneck function $b_{(i,j)}$, as well as an effect function $f_{(i,j)}$. For linear models, we sample $b_{(i,j)}$ by sampling a random matrix $\mathbf{B} \in [0, 1]^{d_{\mathbf{X}} \times d_{\mathbf{Z}}}$ and $f_{(i,j)}$ by sampling a random matrix $\mathbf{F} \in [0, 1]^{d_{\mathbf{Z}} \times d_{\mathbf{X}}}$, both with rank = $d_{\mathbf{Z}}$. For nonlinear models, $b_{(i,j)}$ and $f_{(i,j)}$ are implemented by randomly initialized, multilayer perceptrons (MLPs). Details for each experimental setup are provided in Section D.3. See also Section E for a detailed discussion on sampling nonlinear functions. Unless specified otherwise, by default we use the parameters $|\mathcal{V}| = 10$, $d_{\mathbf{X}} = 5$, $d_{\mathbf{Z}} = 2$ and $n = 30000$ for linear models and $n = 50000$ for nonlinear models, respectively. We conduct experiments where we vary one of these parameters while keeping all others fixed.

D.2. Detailed Estimation Procedure

As per Assumption 2.3, we consider the case where there is a separate bottleneck for each parent of an endogenous node. Graphically, this means there is a bottleneck space for each edge in a model’s graph. Since each edge between variables \mathbf{X}_i and \mathbf{X}_j can be decomposed into a bottleneck function $b_{(i,j)}$, that maps to the corresponding bottleneck space $\mathcal{Z}_{(i,j)}$ and an effect function $f_{(i,j)}$ that maps from the bottleneck space to \mathcal{X}_j , the targets of the estimation procedure are the bottleneck function $b_{(i,j)}$ and the effect function $f_{(i,j)}$. We recover the joint map $m_{(i,j)} := f_{(i,j)} \circ b_{(i,j)} : \mathcal{X}_i \times \mathcal{H}_j \rightarrow \mathcal{X}_j$ by fitting an estimator from \mathbf{X}_i to \mathbf{X}_j . The conditioning sets required for this estimation procedure are analogous to standard causal effect estimation. As our identifiability results presented in Section 4 tell us, from the estimated composed map $\hat{m}_{(i,j)}$ we are able to recover both $b_{(i,j)}$ and $f_{(i,j)}$ up to an invertible map $\psi_{(i,j)}$, i.e., $\hat{b}_{(i,j)} := \psi_{(i,j)} \circ b_{(i,j)}$ and $\hat{f}_{(i,j)} := f_{(i,j)} \circ \psi_{(i,j)}^{-1}$. How $\hat{b}_{(i,j)}$ and $\hat{f}_{(i,j)}$ are recovered from $\hat{m}_{(i,j)}$ is described in detail in the following. Code to reproduce all experimental results is available at <https://github.com/simonbing/StructuralCausalBottleneckModels>. We implement our estimation pipeline using the JAX machine learning library (Bradbury et al., 2018).

Conditioning Sets. The procedure for estimating the bottleneck space corresponding to the edge $\mathbf{X}_i \rightarrow \mathbf{X}_j$ is analogous to estimating the direct effect of \mathbf{X}_i on \mathbf{X}_j . As such, we can use any conditioning set for this estimation that is valid for effect estimation. Given the source node \mathbf{X}_i and target node \mathbf{X}_j , a valid conditioning set is $\{\mathbf{X}_{\text{pa}(i)}, \mathbf{X}_{\text{pa}(j)}\}$. Since bottleneck variables are deterministic transforms of their parent nodes, we can equivalently use the set of (lower dimensional) bottleneck variables $\{(\mathbf{Z}_{(k,i)})_{k \in \text{pa}(i)}, (\mathbf{Z}_{(\ell,j)})_{\ell \in \text{pa}(j)}\}$ for conditioning.

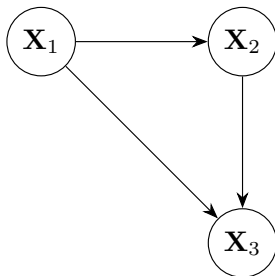


Figure 7. Three-node, fully connected graph.

Linear vs. Nonlinear Estimators. Let $\mathbf{X}_i \in \mathbb{R}^{d_i}$, $\mathbf{X}_j \in \mathbb{R}^{d_j}$ and $\mathbf{Z}_{(i,j)} \in \mathbb{R}^{d_{(i,j)}}$. Fitting an estimator between \mathbf{X}_i and \mathbf{X}_j results in a map $\hat{m}_{(i,j)} : \mathbb{R}^{d_i} \mapsto \mathbb{R}^{d_j}$ from which we must extract the estimates of the bottleneck function $\hat{b}_{(i,j)} : \mathbb{R}^{d_i} \mapsto \mathbb{R}^{d_{(i,j)}}$ and the effect function $\hat{f}_{(i,j)} : \mathbb{R}^{d_{(i,j)}} \mapsto \mathbb{R}^{d_j}$. In the linear case, fitting an estimator returns a weight matrix $\hat{\mathbf{M}} \in \mathbb{R}^{d_i \times d_j}$, which by the assumption of our data generating process has rank $d_{(i,j)} \ll d_i, d_j$. Extracting $\hat{b}_{(i,j)}$ and $\hat{f}_{(i,j)}$ amounts to finding a matrix factorization $\hat{\mathbf{M}} = \hat{\mathbf{B}}_{(i,j)} \hat{\mathbf{F}}_{(i,j)}$, where $\hat{\mathbf{B}}_{(i,j)} \in \mathbb{R}^{d_i \times d_{(i,j)}}$ and $\hat{\mathbf{F}}_{(i,j)} \in \mathbb{R}^{d_{(i,j)} \times d_j}$. We recover $\hat{\mathbf{B}}_{(i,j)}$ by selecting $d_{(i,j)}$ linearly independent columns from $\hat{\mathbf{M}}$ and $\hat{\mathbf{F}}_{(i,j)}$ by computing $\hat{\mathbf{F}}_{(i,j)} = \hat{\mathbf{B}}_{(i,j)}^+ \hat{\mathbf{M}}$, where $(\cdot)^+$ denotes the Moore-Penrose inverse (Moore, 1920; Bjerhammar, 1951; Penrose, 1955). In the case of a nonlinear estimator, we go about this factorization by means of the chosen network architecture. We employ an encoder-decoder structure where we train an encoder network \hat{b}_θ , parametrized by weights θ , to map from the source node \mathbf{X}_i to the bottleneck $\mathbf{Z}_{(i,j)}$ and a decoder network \hat{f}_ϕ , parametrized by weights ϕ , to map from the bottleneck to the target node \mathbf{X}_j .

Estimating All Bottlenecks. If our goal is to estimate *all* bottlenecks in a given SCBM, we need to take special care of the order in which we do this, especially if we plan to use previously estimated bottlenecks as conditioning variables. To illustrate this point, consider the following three-node, fully connected graph, presented in Figure 7. The associated SCBM \mathcal{C} has three bottlenecks: $\mathbf{Z}_{(1,2)}$, $\mathbf{Z}_{(1,3)}$ and $\mathbf{Z}_{(2,3)}$.

As a first approach, let us naively estimate these bottleneck variables in the causal order of their parents. The causal ordering for this example is $(\mathbf{X}_1, \mathbf{X}_2, \mathbf{X}_3)$. Thus, we start by estimating $\mathbf{Z}_{(1,2)}$, for which we fit an estimator $\mathbf{X}_1 \rightarrow \mathbf{X}_2$ without requiring any conditioning. So far, so good. Next up in this order is $\mathbf{Z}_{(1,3)}$. Looking at our graph \mathcal{G} (cf. Figure 7), we see that we need to close the path $\mathbf{X}_1 \rightarrow \mathbf{X}_2 \rightarrow \mathbf{X}_3$, which we want to do with a bottleneck variable. Graphically, we might be tempted to use $\hat{\mathbf{Z}}_{(1,2)}$ from the first step, since this bottleneck variable “lives” on the edge $\mathbf{X}_1 \rightarrow \mathbf{X}_2$, which is part of the path we want to close. However, remembering that bottleneck variables are *deterministic* transformations of their parents, i.e., $\mathbf{Z}_{(i,j)} := b_{(i,j)}(\mathbf{X}_i)$, we see that this is not a valid conditioning set, as it contains the same information as our source \mathbf{X}_1 . A valid conditioning bottleneck for this case would be $\mathbf{Z}_{(2,3)}$, but we have not yet estimated it! This approach clearly does not work, in general.

We propose an alternative approach. First, notice that for any given bottleneck estimation routine we require a source \mathbf{X}_i and a target \mathbf{X}_j . We propose to first loop over candidate target nodes in the causal order implied by the graph \mathcal{G} and then for each target loop over its parents along their *reverse* causal order. Let us return to our example to illustrate how this new approach helps. We begin the outer loop over targets along the causal order: \mathbf{X}_1 is the first candidate target, but since it has no parents (and therefore no ancestral bottlenecks) we skip it and continue with \mathbf{X}_2 . Since \mathbf{X}_1 is the only parent of \mathbf{X}_2 we estimate $\mathbf{Z}_{(1,2)}$ by fitting an estimator between $\mathbf{X}_1 \rightarrow \mathbf{X}_2$. Moving along the causal order the next target is \mathbf{X}_3 with parents $(\mathbf{X}_1, \mathbf{X}_2)$. Progressing along the reverse causal order, we begin with \mathbf{X}_2 as a source node and estimate $\mathbf{Z}_{(2,3)}$. Graphically, we must close the backdoor path $\mathbf{X}_2 \leftarrow \mathbf{X}_1 \rightarrow \mathbf{X}_3$. We can use the estimate $\hat{\mathbf{Z}}_{(1,2)}$ from the previous step as a conditioning variable to do so. What remains is estimating $\mathbf{Z}_{(1,3)}$, and as we noticed in the naïve approach above, this requires conditioning on $\mathbf{Z}_{(2,3)}$. Now it becomes evident why our proposed approach works where the naïve approach fails: all required conditioning bottlenecks have already been estimated in previous steps.

We can generalize this approach to DAGs beyond the simple example discussed above by recalling how a general estimation problem for a bottleneck variable looks like. Estimating a given bottleneck $\mathbf{Z}_{(i,j)}$ is analogous to estimating the direct effect of a given edge $\mathbf{X}_i \rightarrow \mathbf{X}_j$. To this end, we want to block all front- and backdoor paths between source \mathbf{X}_i and target \mathbf{X}_j . Backdoor paths by definition include a parent $\mathbf{X}_{k \in \text{pa}(i)}$ of the source \mathbf{X}_i , so this path can be closed by the bottleneck $\mathbf{Z}_{(k,i)}$. Looping over all targets along the causal order ensures that this bottleneck has been estimated before estimating $\mathbf{Z}_{(i,j)}$.

The inner loop over potential source nodes of a target \mathbf{X}_j occurs along the reverse causal order of the parents of \mathbf{X}_j to ensure that any frontdoor paths can also be closed. All frontdoor paths between source \mathbf{X}_i and target \mathbf{X}_j include a parent $\mathbf{X}_{\ell \in \text{pa}(j)}$ of the target. Beginning with the parent *latest* in the causal order as the candidate source node ensures that there is no other potential frontdoor path open between source and target: if there were, this parent \mathbf{X}_ℓ would have been later in the causal order. Iterating backwards along the causal order ensures that any potential frontdoor paths can be closed using the estimated bottleneck from a previous step.

See Algorithm 1 for pseudocode describing how we estimate all bottleneck (and mechanism) functions of a given SCBM. Notice that the estimate of a bottleneck variable is straightforwardly given by applying the estimated bottleneck function: $\hat{\mathbf{Z}}_{(i,j)} := \hat{b}_{(i,j)}(\mathbf{X}_i)$.

Algorithm 1 Estimate Bottleneck & Effect Functions

Input: SCBM $\mathfrak{C} = \langle \mathcal{G} = (\mathcal{V}, \mathcal{E}), \mathcal{X}, \mathcal{Z}, \mathcal{H}, \boldsymbol{\eta}, \mathcal{B}, \mathcal{F}, \mathbf{X} \rangle$, causal order $C[1..|\mathcal{V}|]$, assumed bottleneck dimension $d_{\hat{\mathbf{Z}}}$

```

for  $j$  in  $C$  do                                     ▷ Outer loop over target nodes.
   $target \leftarrow \mathbf{X}_j$ 
  if  $target$  is root node then
    pass                                               ▷ Root nodes have no bottlenecks.
  else
    for  $i$  in  $\text{reversed}(C[:j])$  do                   ▷ Inner loop over source nodes.
       $source \leftarrow \mathbf{X}_i$ 
       $\hat{\mathbf{Z}}_{cond} \leftarrow \text{GetCondSet}(\mathfrak{C}, i, j)$        ▷ According to procedure described in Appendix D.2.
       $\hat{m}_{(i,j)} \leftarrow \text{fit}(source, target, \hat{\mathbf{Z}}_{cond})$   ▷ Using linear or nonlinear regressor.
       $\hat{b}_{(i,j)}, \hat{f}_{(i,j)} \leftarrow \text{factorize}(\hat{m}_{(i,j)}, d_{\hat{\mathbf{Z}}})$ 
      Cache  $\hat{b}_{(i,j)}, \hat{f}_{(i,j)}$ 
    end for
  end if
end for

```

D.3. Nonlinear SCBMS: Data Generation Details & Hyperparameters

D.3.1. IDENTIFIABILITY

To sample nonlinear bottleneck and effect functions, we randomly initialize MLPs with two hidden layers with $d_{\text{hidden}} = d_{\mathbf{X}}$ and orthogonalize as described in Section E. We use the swish nonlinearity. Hyperparameters of the estimator are described in Table 1.

D.3.2. MISSPECIFICATION

The data generation process and hyperparameters for the misspecification experiments follow those of the identifiability experiments described above.

D.3.3. TRANSFER LEARNING

For the transfer learning experiment we sample nonlinear functions by randomly initialized MLPs with four hidden layers and $d_{\text{hidden}} = d_{\mathbf{X}}$, using ReLU activation functions. We opt for this approach as opposed to the architecture used in the previous experiments as initializing MLPs with an orthogonalization step results in more complex maps that require significantly more training samples to learn (see Section E for a detailed discussion). The advantage of bottleneck variables as conditioning sets in transfer learning settings occur in low sample regimes, but for these more complex functions, irrespective of conditioning choice, performance in the low sample regime was too poor to draw a meaningful comparison. Hyperparameters for these experiments are provided in Table 2.

Table 1. Hyperparameters for identifiability and misspecification experiments.

HYPERPARAMETER	VALUE
ENCODER HIDDEN LAYER SIZES	[256, 128, 64, 64, 32]
DECODER HIDDEN LAYER SIZES	[32, 64, 64, 128, 256]
EPOCHS	500
BATCH SIZE	1024
OPTIMIZER	ADAMW (Loshchilov & Hutter, 2019)
LEARNING RATE SCHEDULER	COSINE DECAY W/ WARMUP
MAX. LEARNING RATE	1e−5
MIN. LEARNING RATE	1e−7
WARMUP STEPS	1000
DECAY STEPS	10000

Table 2. Hyperparameters for the transfer learning experiment.

HYPERPARAMETER	VALUE
ENCODER HIDDEN LAYER SIZES	[128, 128, 128, 128, 128, 128]
DECODER HIDDEN LAYER SIZES	[128, 128, 128, 128, 128, 128]
EPOCHS	500
BATCH SIZE	512
OPTIMIZER	ADAMW (Loshchilov & Hutter, 2019)
LEARNING RATE SCHEDULER	-
LEARNING RATE	5e−6

E. On Randomly Sampling Nonlinear Functions

While visualizing ground-truth bottleneck spaces in nonlinear SCBMs, we stumbled across an unexpected phenomenon: randomly sampled ground-truth bottleneck spaces \mathcal{Z} seemed to collapse to a one-dimensional subspace. Recalling that bottleneck functions map from observed to bottleneck spaces, i.e., $b_{(i,j)} : \mathcal{X}_i \rightarrow \mathcal{Z}_{(i,j)}$, we can see how this phenomenon has its explanation in the choice of ground-truth bottleneck functions. Following common practice, we sample these nonlinear bottleneck functions by randomly initializing MLPs.

A nonlinear function $m_{(i,j)} : \mathbb{R}^{d_i} \rightarrow \mathbb{R}^{d_j}$ is implemented by an MLP with input dimension d_i and output dimension d_j . Such an MLP is nothing more than the product of randomly sampled matrices—all layers with randomly sampled weights—composed with element-wise nonlinearities. Let us disregard the nonlinearities for now and take a closer look at products of random matrices, which we write as

$$M = \prod_{i=1}^h W_i,$$

where, for simplicity, we assume all factors W_i to have compatible dimensions and full column rank. The number of factors h can be understood as the number of hidden layers in the corresponding MLP.

Let $r = \min_{i \in \{1..h\}} \text{rank}(W_i)$ denote the smallest rank of any factor in this product. We know that for the product it holds that $r = \text{rank}(M)$. However, empirically, we observe that the numerical rank of M quickly approaches 1. Quickly, in this context, means that this behaviour is observed for as few as three factors. This phenomenon also seems robust to the base distribution from which entries are chosen, as well as the size of the factor matrices. Understanding and characterizing this behaviour is active work in progress in an orthogonal research project.

While we cannot yet fully explain the origins of this collapse, we do propose an effective remedy in practice. When sampling the random matrices corresponding to individual matrices, we append an orthogonalization step. This is achieved by taking the QR -decomposition of the factor W_i and taking Q as the layer matrix. We thereby guarantee that we have the same span as the originally sampled W_i , but with an orthogonal basis. Empirically, this results in much more numerically stable full-rank products.

The technical difference between our proposed, new approach and the original one (without orthogonalization) is that we have proper control of the dimension of the space to which our MLP maps. Neither of the two is per se right or wrong, but their difference is worth being aware of. Rather, we believe our findings raise the question of how to “properly” sample nonlinear functions in the first place. In our experiments, we see that the orthogonalization approach leads to significantly more complex functions (requiring more samples and resulting in slightly lower identifiability metrics), but how representative such synthetic functions are of practical problems remains an open question.